more critically than do the more malleable ordered phases. The latter can accommodate a wider range of solute shapes and sizes due to their own lower intermolecular ordering. However, once in one of the malleable matrices, even the best-fit solutes experience an environment which is more tolerant of conformational change.

Also, we have noted previously that irradiation of neat solid *n*-alkanones does not result in photoproduct selectivity which is as great as that found when the same ketones are dissolved in solid solutions of *n*-alkanes with the same number of carbon atoms.

Thus, the greatest restriction to motion experienced by an alkanone molecule is not always that afforded by its crystalline matrix nor is it presented by more malleable liquid-crystalline environments. We believe that this conclusion should apply to the reactions of many other solutes.

Acknowledgment. We thank the National Science Foundation for its support of this work and Dr. Patricia Vilalta for helpful discussions. A.N. acknowledges the Consejo Nacional de Investigaciones Cientificas y Tecnicas de la Republica de la Argentina for a travel grant.

Electron-Transfer Oxidation of Ketene Silyl Acetals and Other Organosilanes. The Mechanistic Insight into Lewis Acid Mediated Electron Transfer

Shunichi Fukuzumi,*,† Morifumi Fujita,† Junzo Otera,*,‡ and Yukihiro Fujita‡

Contribution from the Department of Applied Chemistry, Faculty of Engineering, Osaka University, Suita, Osaka 565, Japan, and Department of Applied Chemistry, Okayama University of Science, Ridai-cho, Okayama 700, Japan. *Received April 27, 1992*

Abstract: Kinetic studies on photoinduced and thermal electron-transfer oxidation of a variety of organosilanes in acetonitrile at 298 K are reported in terms of the electron-transfer rate constants (k_{et}) with a series of oxidants having the known one-electron reduction potentials (E^0_{red}). The Rehm–Weller Gibbs energy relationship is applied to determine the fundamental parameters for the electron-transfer oxidation, i.e., the one-electron oxidation potentials (E^0_{ox}) and the intrinsic barrier for the electron-transfer oxidation ($\Delta G^{\ddagger}_0$). The E^0_{ox} and $\Delta G^{\ddagger}_0$ values thus obtained are compared with the calculated values of the adiabatic ionization potentials (I_a) and the inner-sphere reorganization energies (λ_i) associated with the structural change upon electron-transfer oxidation by using the PM3 molecular orbital method. Ketene silyl acetals, especially hindered ones, are shown to act as unique and strong electron donors as compared to other organosilanes. On the other hand, Lewis acids such as $SnCl_4$, Ph_3SiClO_4, and Et_3SiClO_4, which catalyze the addition of hindered ketene acetals to α-enones, are shown to act as strong electron acceptors in the electron-transfer oxidation of ferrocene derivatives. The mechanistic insight to the electron-transfer oxidation of organosilanes, particularly in the case of hindered ketene silyl acetals which are employed in Lewis acid promoted carbon–carbon bond formation reactions, is discussed on the basis of the fundamental parameters for the electron-transfer oxidation.

Introduction

Organosilanes have been frequently used as key reagents for many synthetically important transformations. Lewis acid promoted carbon–carbon bond formation reactions of organosilanes such as allylsilanes, enol silyl ethers, and ketene silyl acetals expecially have been of considerable interest in organic synthesis in recent years.[1] Quantitative information on the reactivities of allylsilanes and enol silyl ethers acting as nucleophiles has recently been derived from the kinetic investigations on the reactions of diarylcarbenium ions with these important organosilanes.[2] On the other hand, electron-transfer oxidation of organosilanes has also been receiving increased attention recently in both thermal[3,4] and photochemical[5-7] reactions. However, the fundamental properties such as the one-electron oxidation potentials (E^0_{ox}) and the intrinsic barrier for the electron-transfer oxidation of organosilanes have, to the best of our knowledge, not yet been available.

We report herein the kinetic investigations on both the photoinduced and thermal electron-transfer oxidation of various organosilanes to determine the E^0_{ox} and $\Delta G^{\ddagger}_0$ values that would otherwise be difficult to obtain.[8] The E^0_{ox} and $\Delta G^{\ddagger}_0$ values thus obtained are compared with those predicted by the molecular orbital calculations. In addition, we determined the rate constants of the electron-transfer reduction of some Lewis acids that are frequently used as promoters for the C–C bond formation reactions. These data provide the energetic basis for the Lewis acid mediated electron-transfer processes of organosilanes as well as

† Osaka University.
‡ Okayama University of Science.

(1) (a) Colvin, E. W. *Silicon in Organic Synthesis*; Butterworths: London, 1981. (b) Mukaiyama, T. *Angew. Chem., Int. Ed. Engl.* **1977**, *16*, 817. (c) Mukaiyama, T.; Murakami, M. *Synthesis* **1987**, 1043. (d) Gennari, C. *Selectivities in Lewis Acid Promoted Reactions*; Schinzer, D., Ed.; Kluwer Academic Publishers: Dordrecht, The Netherlands, 1989; Chapter 4, p 53. (e) Heathcock, C. H. *Aldrichimica Acta* **1990**, *23*, 99.

(2) (a) Bartl, J.; Steenken, S.; Mayr, H. *J. Am. Chem. Soc.* **1991**, *113*, 7710. (b) Hagen, G.; Mayr, H. *J. Am. Chem. Soc.* **1991**, *113*, 4954. (c) Mary, H. *Angew. Chem., Int. Ed. Engl.* **1990**, *29*, 1371.

(3) (a) Reetz, M. T.; Schwellnus, K.; Hübner, F.; Massa, W.; Schmidt, R. E. *Chem. Ber.* **1983**, *116*, 3708. (b) Baciocchi, E.; Casu, A.; Ruzziconi, R. *Tetrahedron Lett.* **1989**, *30*, 3707. (c) Snider, R. B.; Kwon, T. *J. Org. Chem.* **1990**, *55*, 4786. (d) Ali, S. M.; Rousseau, G. *Tetrahedron* **1990**, *46*, 7011. (e) Totten, C. E.; Wenke, G.; Karydas, A. C.; Rhodes, Y. E. *Synth. Commun.* **1985**, *15*, 301. (f) Bhattacharya, A.; DiMichele, L. M.; Dolling, U.-H.; Grabowski, E. J. J.; Grenda, V. J. *J. Org. Chem.* **1989**, *54*, 6118. (g) Yoshida, J.; Maekawa, T.; Murata, T.; Matsunaga, S.; Isoe, S. *J. Am. Chem. Soc.* **1990**, *112*, 1962. (h) Fukuzumi, S.; Kitano, T.; Mochida, K. *J. Am. Chem. Soc.* **1990**, *112*, 3246.

(4) A number of stable organosilicon radical cations have been reported: Kaim, W. *Acc. Chem. Res.* **1985**, *18*, 160 and references cited therein.

(5) Mariano, P. S. *Photoinduced Electron Transfer*; Fox, M. A., Chanon, M., Eds.; Elsevier: Amsterdam, 1988; Part C, p 372 and references cited therein.

(6) (a) Gassman, P. G.; Hay, B. A. *J. Am. Chem. Soc.* **1986**, *108*, 4227. (b) Gassman, P. G.; Hay, B. A. *J. Am. Chem. Soc.* **1985**, *107*, 4075. (c) Gassman, P. G.; Bottorff, K. J. *J. Org. Chem.* **1988**, *53*, 1097. (d) Dinnocenzo, J. P.; Farid, S.; Goodman, J. L.; Gould, I. R.; Todd, W. P.; Mattes, S. L. *J. Am. Chem. Soc.* **1989**, *111*, 8973.

0002-7863/92/1514-10271$03.00/0

valuable insight into the mechanistic viability.

Experimental Section

Materials. Ketene silyl acetals and prenyltrimethylsilane were prepared as described in the literature.[9] Benzyl- and allyltrimethylsilanes are commercially available. Inorganic oxidants used in this study, tris(2,2′-bipyridine)ruthenium(II) dichloride hexahydrate ($[Ru(bpy)_3]Cl_2 \cdot 6H_2O$)[10] and tris(1,10-phenanthroline)iron(III) hexafluorophosphate ($[Fe(phen)_3](PF_6)_3$),[11] were prepared according to the literature. Inorganic reductants used in this study, ferrocene, 1,1′-dimethylferrocene, and decamethylferrocene, were obtained commercially. Organic oxidants (9,10-dicyanoanthracene, naphthalene, pyrene, 2,3-dichloro-5,6-dicyano-*p*-benzoquinone) were also obtained commercially and purified by the standard method.[12] Organometallic oxidants (ferrocenium and 1,1′-dimethylferrocenium ions) were prepared by the oxidation of the corresponding ferrocene derivatives with *p*-benzoquinone in the presence of perchloric acid in acetonitrile[13] and isolated as the hexafluorophosphate salts. The triorganosilyl perchlorate was made by mixing the appropriate triorganosilane with an equivalent amount of triphenylmethyl perchlorate in CH_2Cl_2.[14] Acetonitrile was purified and dried with calcium hydride by the standard procedure[12] and stored under nitrogen atmosphere.

Luminescence Quenching. Quenching experiments of the fluorescence of 10-methylacridinium ion, 9,10-dicyanoanthracene, naphthalene, pyrene, and the $Ru(bpy)_3^{2+}$ luminescence were performed using a Hitachi 650-10S fluorescence spectrophotometer. The excitation wavelengths were 358, 390, 300, 365, and 450 nm for 10-methylacridinium ion, 9,10-dicyanoanthracene, naphthalene, pyrene, and $Ru(bpy)_3^{2+}$ in MeCN, respectively. The monitoring wavelengths were those corresponding to the maxima of the respective emission bands at 487, 460, 335, 420, and 608 nm. The solutions were deoxygenated by argon purging for 10 min prior to the measurements. Relative emission intensities were measured for MeCN solutions of each sensitizer with an organosilane quencher at various concentrations. There was no change in the shape but there was a change in the intensity of the fluorescence spectrum by the addition of a quencher. The Stern–Volmer relationship (eq 1) was obtained for the

$$I_0/I = 1 + K_{SV}[D] \quad (1)$$

ratio of the emission intensities in the absence and presence of an electron donor (I_0/I) and the concentrations of donors used as quenchers [D]. In the case of fluorescence quenching of naphthalene by some quenchers, the Stern–Volmer plot showed a deviation from a linear correlation between I_0/I and [D] in the high concentrations of donors which absorb light at the excitation wavelength. In such a case, the longer excitation wavelength (e.g., λ = 340 nm) was selected, and the quenching constant was determined from the initial slope of the Stern–Volmer plot. The fluorescence lifetime τ of $AcrH^+$ was determined as 31 ns in MeCN by single photon counting using a Horiba NAES-1100 time-resolved spectrofluorophotometer. The observed quenching rate constants k_q (= $K_{SV}\tau^{-1}$) were obtained from the Stern–Volmer constants K_{SV} and the emission lifetimes τ.

Kinetic Measurements. Kinetic measurements were performed under deaerated conditions using a Union RA-103 stopped-flow spectrophotometer and a Union SM-401 spectrophotometer for fast reactions with half-lives shorter than 10 s and for the slower reactions with half-lives much longer than 10 s, respectively. Rates of the electron-transfer reactions from electron donors to $Fe(phen)_3^{3+}$ in MeCN containing an excess amount of an organosilane were followed by the increase in absorbance at λ_{max} = 507 nm due to $Fe(phen)_3^{2+}$.[11] Rates of the electron-transfer reactions from organosilanes to 2,3-dichloro-5,6-dicyano-*p*-benzoquinone (DDQ) and ferrocenium ion derivatives in MeCN were followed by the decrease in absorbance due to DDQ and the corresponding ferrocenium ions in the long-wavelength region (600–700 nm), respectively.[13] Rates of the electron-transfer reactions from ferrocene derivatives to Lewis acids in CH_2Cl_2 were also followed by the increase in absorbance due to the corresponding ferrocenium ions in the long-wavelength region (λ = 600–700 nm).[13] All of the kinetic measurements were carried out under the pseudo-first-order conditions by using more than 10-fold excess reductants at 298 K. Pseudo-first-order rate constants were determined by a least-squares curve fit using a Union System 77 microcomputer.

Cyclic Voltammetry. The cyclic voltammetry measurements were performed on a Hokuto Denko Model HA-301 potentiostat–galvanostat in deaerated MeCN containing 0.10 M Bu_4NClO_4 as a supporting electrolyte at 298 K. The measured potentials were recorded with respect to the saturated calomel electrode (SCE). The platinum microelectrode was routinely cleaned by soaking it in concentrated nitric acid, followed by repeated rinsing with water and acetone and drying at 353 K prior to use in order to avoid possible fouling of the electrode surface. The cyclic voltammograms of ketene silyl acetals exhibit the irreversible anodic waves at relatively low potentials (ca. 0.8–1.0 V) as compared to that of tetraethylsilane (>2.0 V). Unfortunately, however, the rapid decrease in the anodic current due to hydration of ketene silyl acetals occurring during the measurements has precluded the detailed analysis of the anodic waves.

Theoretical Calculations. The theoretical studies were performed using the PM3 or MNDO molecular orbital method.[15,16] The MOPAC program (QCPE No. 455), which was revised as OS/2 Version 5.01 to adapt it for use on a NEC PC computer, was obtained through the Japan Chemistry Program Exchange (JCPE).[17] The structural output was recorded by using the MOPC program (JCPE No. P038). Final geometries and energetics were obtained by optimizing the total molecular energy with respect to all structural variables. The geometries of the radical cations were optimized using unrestricted Hartree–Fock (UHF) formalism. The adiabatic ionization potentials (I_a) were calculated as the difference in the heat of formation (ΔH_f) between the radical cation and the corresponding neutral form, when the ΔH_f values of the radical cations were calculated with the UHF-optimized structures using the half-electron (HE) method with restricted Hartree–Fock (RHF) formalism.[18] The reorganization energies of the inner coordination spheres (λ_i) associated with the structural change of organosilanes upon electron-transfer oxidation were calculated as the difference in ΔH_f of the radical cations with the same structures as the neutral forms and ΔH_f with the optimized structures using UHF formalism.

Results and Discussion

Electron-Transfer Oxidation of Organosilanes. Since direct electrochemical measurements of ketene silyl acetals were complicated by irreversible behavior as well as by the hydration occurring upon oxidation (see the Experimental Section), we have examined the rates of outer-sphere electron-transfer oxidation from which the fundamental one-electron oxidation properties can be deduced (vide infra).

The significant increase in the acceptor ability of electron acceptors by electronic excitation is well-known to result in electron-transfer quenching of the excited states of acceptors by the ground-state donors.[19,20] Rehm and Weller[19] have formulated the following reaction scheme for emission quenching by electron transfer from an electron donor (D) to the excited-state acceptor (A^*) in MeCN as shown in eq 2, where k_{12} and k_{21} are the

$$D + A^* \underset{k_{21}}{\overset{k_{12}}{\rightleftharpoons}} (DA^*) \underset{k_{32}}{\overset{k_{23}}{\rightleftharpoons}} (D^+A^{\bullet-}) \xrightarrow{k_{30}} D + A \quad (2)$$

(7) (a) Sakurai, H.; Sakamoto, K.; Kira, M. *Chem. Lett.* **1984**, 1213. (b) Nakadaira, Y.; Komatsu, N.; Sakurai, H. *Chem. Lett.* **1985**, 1781. (c) Mizuno, K.; Ikeda, M.; Otsuji, Y. *Tetrahedron Lett.* **1985**, *26*, 461. (d) Mizuno, K.; Kobata, T.; Maeda, R.; Otsuji, Y. *Chem. Lett.* **1990**, 1821. (e) Fukuzumi, S.; Kitano, T.; Mochida, K. *Chem. Lett.* **1989**, 2177. (f) Fukuzumi, S.; Kitano, T.; Mochida, K. *Chem. Lett.* **1990**, 1774. (g) Fukuzumi, S.; Kitano, T.; Mochida, K. *J. Chem. Soc., Chem. Commun.* **1990**, 1236.

(8) A preliminary report has appeared: Sato, T.; Wakahara, Y.; Otera, J.; Nozaki, H.; Fukuzumi, S. *J. Am. Chem. Soc.* **1991**, *113*, 4028.

(9) (a) Ireland, R. E.; Wipf, P.; Armstrong, J. D., III *J. Org. Chem.* **1991**, *56*, 650. (b) Gennari, C.; Beretta, M. G.; Bernardi, A.; Moro, G.; Scolastico, C.; Todeschini, R. *Tetrahedron* **1986**, *42*, 893. (c) Hosomi, A.; Shirahata, A.; Sakurai, H. *Chem. Lett.* **1978**, 901.

(10) Burstall, F. H. *J. Chem. Soc.* **1936**, 173.

(11) (a) Fukuzumi, S.; Nishizawa, N.; Tanaka, T. *Bull. Chem. Soc. Jpn.* **1982**, *55*, 3482. (b) Ford-Smith, M. H.; Sutin, N. *J. Am. Chem. Soc.* **1961**, *83*, 1830.

(12) Perrin, D. D.; Armarego, W. L. F.; Perrin, D. R. *Purification of Laboratory Chemicals*; Pergamon Press: New York, 1966.

(13) (a) Ishikawa, K.; Fukuzumi, S.; Goto, T.; Tanaka, T. *J. Am. Chem. Soc.* **1990**, *112*, 1578. (b) Fukuzumi, S.; Ishikawa, K.; Hironaka, K.; Tanaka, T. *J. Chem. Soc., Perkin Trans. 2* **1987**, 751.

(14) Lambert, J. B.; McConnell, J. A.; Shilf, W.; Schulz, W. J., Jr. *J. Chem. Soc., Chem. Commun.* **1988**, 455.

(15) Stewart, J. J. P. *J. Comput. Chem.* **1989**, *10*, 209, 221.

(16) (a) Dewar, M. J. S.; Thiel, W. *J. Am. Chem. Soc.* **1977**, *99*, 4899. (b) Dewar, M. J. S.; Thiel, W. *J. Am. Chem. Soc.* **1977**, *99*, 4907.

(17) Toyoda, J. *JCPE News Lett.* **1990**, *2*, 37.

(18) Clark, T. *A Handbook of Computational Chemistry*; Wiley: New York, 1985; p 97.

(19) (a) Rehm, A.; Weller, A. *Ber. Bunsenges. Phys. Chem.* **1969**, *73*, 834. (b) Rehm, A.; Weller, A. *Isr. J. Chem.* **1970**, *8*, 259.

(20) (a) Julliard, M.; Chanon, M. *Chem. Rev.* **1983**, *83*, 425. (b) Chanon, M.; Hawley, M. D.; Fox, M. A. *Photoinduced Electron Transfer*; Chanon, M., Fox, M. A., Eds.; Elsevier: Amsterdam, 1988; Part A, p 1.

diffusion and dissociation rate constants in the encounter complex (DA^*), k_{23} and k_{32} are the rate constants of forward electron transfer from D to A* and back electron transfer to the excited state, respectively, and k_{30} is the rate constant of back electron transfer to the ground state. The overall rate constant (k_{et}) of the emission quenching by electron transfer is given by eq 3, which is reduced to eq 4 under the conditions that the back electron transfer to the ground state is much faster than that to the excited state, i.e., $k_{30} \gg k_{32}$.[21,22] From eq 4 is derived eq 5, where $\Delta G^{\ddagger}$

$$k_{et} = k_{12}k_{23}/[k_{23} + k_{21}(1 + k_{32}/k_{30})] \quad (3)$$

$$k_{et} = k_{12}k_{23}/(k_{23} + k_{21}) \quad (4)$$

is the activation Gibbs energy of the bimolecular electron-transfer process ($k_{23}k_{12}/k_{21}$), Z is the collision frequency that is taken as 1×10^{11} M^{-1} s^{-1}, F is the Faraday constant, the k_{12} value in MeCN is 2.0×10^{10} M^{-1} s^{-1}, and the other notation is conventional.[19,20]

$$\Delta G^{\ddagger} = (2.3RT/F) \log [Z(k_q^{-1} - k_{12}^{-1})] \quad (5)$$

The dependence of $\Delta G^{\ddagger}$ on the Gibbs energy change of electron transfer (ΔG^0_{et}) has been well established as given by the Rehm–Weller Gibbs energy relation (eq 6),[19] where $\Delta G^{\ddagger}_0$ is the intrinsic barrier that represents the activation Gibbs energy when the driving force of electron transfer is zero, i.e., $\Delta G^{\ddagger} = \Delta G^{\ddagger}_0$ at $\Delta G^0_{et} = 0$. On the other hand, the ΔG^0_{et} values are obtained from

$$\Delta G^{\ddagger} = (\Delta G^0_{et}/2) + [(\Delta G^0_{et}/2)^2 + (\Delta G^{\ddagger}_0)^2]^{1/2} \quad (6)$$

the one-electron oxidation potential of the donor (E^0_{ox}) and the one-electron reduction potential of the excited state of the acceptor (E^0_{red}) by using eq 7. From eqs 6 and 7 is derived a linear relation

$$\Delta G^0_{et} = F(E^0_{ox} - E^0_{red}) \quad (7)$$

between $\Delta G^{\ddagger} - \Delta G^0_{et}$ and $(\Delta G^{\ddagger})^{-1}$, as shown in eq 8.[23] The $\Delta G^{\ddagger}$ values are obtained from the quenching rate constants of electron transfer to acceptors (k_{et}) by using eq 5. We can choose appropriate acceptors whose E^0_{red} values are known or readily determined. Thus, the unknown values of E^0_{ox} and $\Delta G^{\ddagger}_0$ can be determined from the intercept and slope of the plots of $\Delta G^{\ddagger} + E^0_{red}$ vs $(\Delta G^{\ddagger})^{-1}$ by using eq 8, respectively.

$$(\Delta G^{\ddagger}/F) + E^0_{red} = E^0_{ox} + (\Delta G^{\ddagger}_0/F)^2/(\Delta G^{\ddagger}/F) \quad (8)$$

The Marcus Gibbs energy relation (eq 9) has also been used in many cases to analyze outer-sphere electron-transfer reactions.[24,25] It is well-known, however, that eq 9 cannot be applied

$$\Delta G^{\ddagger} = \Delta G^{\ddagger}_0[1 + \Delta G^0_{et}/(4\Delta G^{\ddagger}_0)]^2 \quad (9)$$

to forward electron transfer in the largely exothermic region (eq 9 predicts an increase in the $\Delta G^{\ddagger}$ value as ΔG^0_{et} decreases in the region $\Delta G^0_{et} < -4\Delta G^{\ddagger}_0$ (inverted region)), but no such behavior has been reported for forward electron transfer processes although the inverted region has frequently been found for the back electron transfer processes.[26] In addition, from an empirical point of view the use of the Rehm–Weller relation (eq 6) is preferable to the Marcus relation (eq 9), since the linear plot based on eq 8 derived from the Rehm–Weller relation directly yields both the E^0_{ox} and $\Delta G^{\ddagger}_0$ values from the intercepts and slopes.[23]

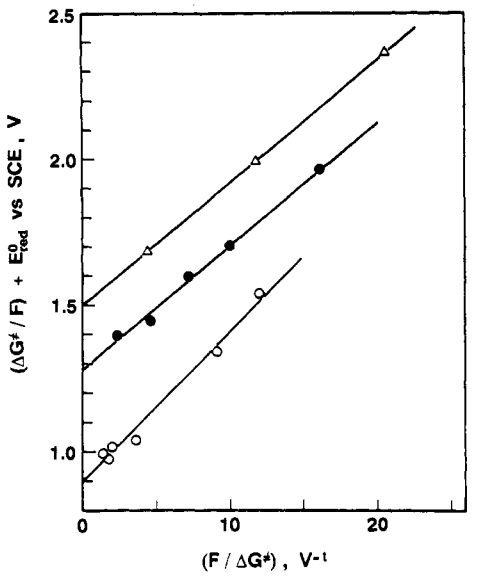

Figure 1. Plots of $(\Delta G^{\ddagger}/F) + E^0_{red}$ vs $F/\Delta G^{\ddagger}$ for electron-transfer oxidation of organosilanes $Me_2C{=}C(OMe)OSiMe_3$ (○), $H_2C{=}C(OEt)OSiMe_3$ (●), and $H_2C{=}CHCH_2SiMe_3$ (△) with various oxidants, based on eq 8.

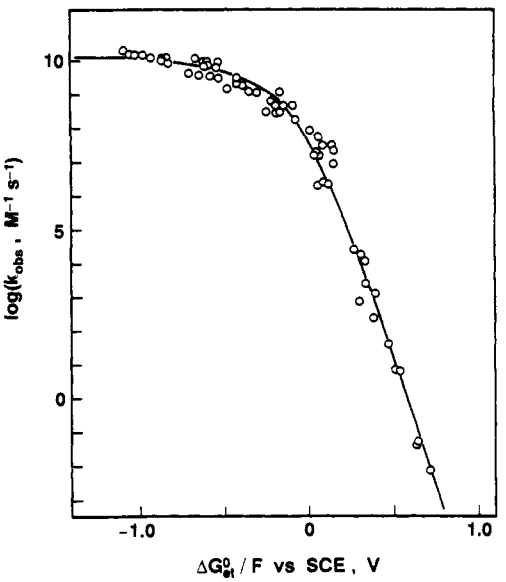

Figure 2. Dependence of log k_{et} on ΔG^0_{et} for electron-transfer oxidation of organosilanes with various one-electron oxidants in MeCN at 298 K. The solid line is drawn according to eqs 5–7, using the E^0_{ox} values and the averaged $\Delta G^{\ddagger}_0$ value (4.6 kcal mol^{-1}) listed in Table II.

A number of rate constants (k_{et}) of photoinduced electron transfer from ketene silyl acetals and other organosilanes to the singlet excited states of electron acceptors (9,10-dicyanoanthracene, naphthalene, pyrene, and $Ru(bpy)_3^{2+}$) are determined by the emission quenching in deaerated MeCN at 298 K (see the Experimental Section). The k_{et} values and the known E^0_{red} values of the excited states[27] are listed in Table I.[28] The k_{et} values of dimethyl-substituted ketene silyl acetals, $Me_2C{=}C(OR^1)OSiR^2_3$ (R^1, R^2 = Me, Et, nos. 1–3 in Table I) and the trimethylsilyl enol

(21) The photoinduced electron-transfer reactions examined in this study are exergonic or slightly endergonic, while the back electron transfer to the ground state is highly exergonic. In such a case, the reversible exciplex formation[22] is unlikely to occur. Moreover, the relation (eq 8) derived under the assumption that $k_{30} \gg k_{32}$ is well verified experimentally as shown in Figure 1, where the data of the thermal electron-transfer reactions are also included.

(22) Gordon, M.; Ware, W. R. *The Exciplex*; Academic Press: New York, 1975.

(23) Fukuzumi, S.; Hironaka, K.; Nishizawa, N.; Tanaka, T. *Bull. Chem. Soc. Jpn.* **1983**, *56*, 2220.

(24) (a) Marcus, R. A. *J. Phys. Chem.* **1963**, *67*, 853. (b) Marcus, R. A. *Annu. Rev. Phys. Chem.* **1964**, *15*, 155.

(25) Eberson, L. *Adv. Phys. Org. Chem.* **1982**, *18*, 79.

(26) For recent reports on the experimental verification of the Marcus inverted region, see: (a) Fox, L. S.; Kozik, M.; Winkler, J. R.; Gray, H. B. *Science* **1990**, *247*, 1069. (b) Gould, I. R.; Ege, D.; Moser, J. E.; Farid, S. *J. Am. Chem. Soc.* **1990**, *112*, 4290 and references cited therein.

(27) (a) Baggott, J. E.; Pilling, M. J. *J. Chem. Soc., Faraday Trans. 1* **1983**, *79*, 221. (b) Eriksen, J.; Foote, C. S. *J. Phys. Chem.* **1978**, *82*, 2659. (c) Bock, C. R.; Connor, J. A.; Gutierrez, A. R.; Meyer, T. J.; Whitten, D. G.; Sullivan, B. P.; Nagle, J. K. *J. Am. Chem. Soc.* **1979**, *101*, 4815.

(28) The k_{et} value of electron transfer from $H_2C{=}CHCH_2SiMe_3$ (no. 18) to the singlet excited state of the 10-methylacridinium ion ($E^0_{red} = 2.32$ V)[7g] is also included in Table I.

Table I. Observed Second-Order Rate Constants k_{et} for Electron-Transfer Oxidation of Various Organosilanes with One-Electron Oxidants in MeCN at 298 K and One-Electron Reduction Potentials (E^0_{red}) of Oxidants

		k_{et}[a] (M^{-1} s^{-1}) of oxidant[b]					
no.	organosilane	9,10-dicyano-anthracene* (1.91 V)	naphthalene* (1.46 V)	pyrene* (1.23 V)	$Fe(phen)_3^{3+}$ (0.98 V)	$Ru(bpy)_3^{2+}$* (0.77 V)	$Fe(C_5H_5)_2^+$ (0.37 V)
1	$Me_2C{=}C(OEt)OSiMe_3$	2.2×10^{10}	3.5×10^9	1.8×10^9	*d*	2.0×10^6	3.8×10^1
2	$Me_2C{=}C(OEt)OSiEt_3$	1.6×10^{10}	3.8×10^9	1.4×10^9	*d*	2.5×10^6	6.7
3	$Me_2C{=}C(OMe)OSiMe_3$[c]	1.5×10^{10}	3.3×10^9	1.3×10^9	*d*	2.3×10^6	6.1
4	1-methylcyclohexene trimethylsilyl enol ether	1.5×10^{10}	2.8×10^9	1.1×10^9	*d*	*e*	*f*
5	$Me_2C{=}C(O^tBu)OSiMe_2{}^tBu$	1.2×10^{10}	1.4×10^9	2.7×10^8	*f*	*e*	5.0×10^{-2}
6	(*E*)-$Me(H)C{=}C(OEt)OSiEt_3$	1.0×10^{10}	3.5×10^9	1.0×10^9	*d*	*e*	*f*
7	(*E*)-$Me(H)C{=}C(O^tBu)OSiMe_2{}^tBu$	1.1×10^{10}	1.8×10^9	4.9×10^8	*f*	*e*	7.0×10^{-3}
8	$Me_2C{=}C(S^tBu)OSiMe_3$	1.3×10^{10}	6.3×10^8	9.3×10^7	2.4×10^4	*e*	*f*
9	cyclohexene trimethylsilyl enol ether	1.0×10^{10}	1.2×10^9	5.6×10^7	*f*	*e*	*f*
10	$H_2C{=}C(Ph)OSiMe_3$	1.0×10^{10}	*f*	3.3×10^7	1.2×10^4	*e*	*g*
11	$H_2C{=}C(O^tBu)OSiMe_2{}^tBu$	7.2×10^9	4.5×10^8	3.1×10^7	2.4×10^3	*e*	*f*
12	$H_2C{=}C(OEt)OSiMe_3$	6.2×10^9	4.4×10^8	2.0×10^7	7.0×10^3	*e*	*g*
13	$H_2C{=}C(S^tBu)OSiMe_3$	1.0×10^{10}	5.3×10^8	3.4×10^7	1.2×10^3	*e*	*f*
14	$H_2C{=}C(OEt)OSiEt_3$	6.6×10^9	2.8×10^8	1.6×10^7	1.8×10^4	*e*	*g*
15	$H_2C{=}C(^tBu)OSiMe_3$	5.5×10^9	7.3×10^7	1.6×10^7	1.9×10^3	*e*	*g*
16	$Me_2C{=}CHCH_2SiMe_3$	9.0×10^9	1.8×10^8	2.3×10^7	*f*	*e*	*f*
17	$PhCH_2SiMe_3$	6.7×10^9	*f*	9.1×10^6	*f*	*e*	*f*
18	$H_2C{=}CHCH_2SiMe_3$[h]	3.1×10^9	1.5×10^7	*e*	*f*	*e*	*f*

[a] The experimental errors are within ±10%. [b] The E^0_{red} values of oxidants (9,10-dicyanoanthracene*, naphthalene*, pyrene*, $Fe(phen)_3^{3+}$, $Ru(bpy)_3^{2+}$*, $Fe(C_5H_5)_2^+$)[27,29] are shown in parentheses; * denotes the excited states. [c] The k_{et} values of 2,3-dihydro-5,6-dicyano-*p*-benzoquinone (E^0_{red} = 0.51 V) and $Fe(MeC_5H_4)_2^+$ (E^0_{red} = 0.26 V) are determined as 2.4×10^2 and 3.9×10^{-2} M^{-2} s^{-1}, respectively. [d] Too fast to be determined accurately by the stopped-flow technique (>1×10^6 M^{-1} s^{-1}). [e] Below the detection limit of emission quenching (≪1×10^6 M^{-1} s^{-1}). [f] Not determined. [g] Too slow to be determined accurately. [h] The k_{et} value of the singlet excited state of 10-methylacridinium ion (E^0_{red} = 2.32 V)[7g] is 1.2×10^{10} M^{-1} s^{-1}.

ether of 1-methyl-1-cyclohexene (no. 4), are substantially large compared with nonsubstituted ones (nos. 9, 12, and 14).

The strong electron-donor properties of the $Me_2C{=}C(OR^1)OSiR^2_3$ are further demonstrated by the fact that they can transfer an electron thermally to rather mild oxidants such as ferrocenium ion derivatives [$Fe(C_5H_5)_2^+$ and $Fe(MeC_5H_4)_2^+$] as well as $Fe(phen)_3^{3+}$. The rates of electron transfer can be readily followed by the disappearance of the absorbance due to ferrocenium ions and $Fe(phen)_3^{2+}$, showing first-order dependence on the concentration of each reactant. The second-order rate constants k_{et} for the thermal electron transfer in MeCN at 298 K are also summarized in Table I, together with the E^0_{red} values of oxidants.[29]

The unknown values of E^0_{ox} and $\Delta G^{\ddagger}_0$ of various organosilanes are determined from the linear plots of $\Delta G^{\ddagger} + E^0_{red}$ vs $(\Delta G^{\ddagger})^{-1}$ by using eq 8. The typical plots are shown in Figure 1, where the significant difference in the E^0_{ox} values among a β,β-dimethyl-substituted ketene silyl acetal ($Me_2C{=}C(OMe)OSiMe_3$), an unsubstituted one ($H_2C{=}C(OEt)OSiMe_3$), and trimethylallylsilane is readily recognized as the difference in the intercept values. The E^0_{ox} and $\Delta G^{\ddagger}_0$ values of various organosilanes obtained from the intercepts and slopes by least-squares analysis are summarized in Table II.[30,31] The validity of the E^0_{ox} and $\Delta G^{\ddagger}_0$ values thus determined is demonstrated as the plot of log k_{et} vs ΔG^0_{et} in Figure 2, which exhibits a typical feature of the electron-transfer process: the log k_{et} value increased with a decrease in the ΔG^0_{et} value to reach a plateau value corresponding to the diffusion rate constant.

An important point to note from Table II is that the β-methyl substitution of ketene silyl acetals results in a significant decrease in the E^0_{ox} value (1.28, 1.05, and 0.83 V for $H_2C{=}C(OEt)OSiMe_3$ (no. 12), (*E*)-$Me(H)C{=}C(OEt)OSiEt_3$ (no. 6), and $Me_2C{=}C(OEt)OSiMe_3$ (no. 1), respectively). This may be ascribed to the electron-donating effect of methyl groups through hyperconjugation. Such a decrease in the E^0_{ox} value by β-methyl substitution is also observed for the trimethylsilyl enol ether of cyclohexanone

Table II. One-Electron Oxidation Potentials (E^0_{red}) of Various Organosilanes and Intrinsic Barriers of Electron Transfer ($\Delta G^{\ddagger}_0$)

no.	organosilane	E^0_{ox} vs SCE, V	$\Delta G^{\ddagger}_0$, kcal mol^{-1}
1	$Me_2C{=}C(OEt)OSiMe_3$	0.83	5.4
2	$Me_2C{=}C(OEt)OSiEt_3$	0.87	5.2
3	$Me_2C{=}C(OMe)OSiMe_3$	0.90	5.2
4	1-methylcyclohexene trimethylsilyl enol ether	0.94	5.2[a]
5	$Me_2C{=}C(O^tBu)OSiMe_2{}^tBu$	1.01	5.6
6	(*E*)-$Me(H)C{=}C(OEt)OSiEt_3$	1.05	4.5
7	(*E*)-$Me(H)C{=}C(O^tBu)OSiMe_2{}^tBu$	1.08	4.9
8	$Me_2C{=}C(S^tBu)OSiMe_3$	1.25	4.6
9	cyclohexene trimethylsilyl enol ether	1.30	3.8
10	$H_2C{=}C(Ph)OSiMe_3$	1.32	3.7
11	$H_2C{=}C(O^tBu)OSiMe_2Bu^t$	1.32	4.4
12	$H_2C{=}C(OEt)OSiMe_3$	1.28	4.8
13	$H_2C{=}C(S^tBu)OSiMe_3$	1.38	3.6
14	$H_2C{=}C(OEt)OSiEt_3$	1.30	4.6
15	$H_2C{=}C(^tBu)OSiMe_3$	1.34	4.8
16	$Me_2C{=}CHCH_2SiMe_3$	1.39	3.8
17	$PhCH_2SiMe_3$	1.38	4.1
18	$H_2C{=}CHCH_2SiMe_3$	1.50	4.7

[a] Assumed to be the same as that of $Me_2C{=}C(OMe)OSiMe_3$.

(nos. 4 and 9). Another interesting point to note is that the replacement of OEt by S^tBu on β,β-dimethyl ketene silyl acetals results in a significant increase in the E^0_{ox} value (0.83 and 1.25 V for $Me_2C{=}C(OEt)OSiMe_3$ (no. 1) and $Me_2C{=}C(S^tBu)OSiMe_3$ (no. 8), respectively). The replacement of OR and SiR_3 (R = Me or Et) by O^tBu and $SiMe_2{}^tBu$ also causes a increase in the E^0_{ox} value (0.83 and 1.01 V for no. 1 and no. 5). It should also be noted that the $\Delta G^{\ddagger}_0$ values (4.6 ± 0.6 kcal mol^{-1}) of organosilanes are uniformly large compared with those of ordinary π-organic donors (ca. 2 kcal mol^{-1}).[19] Such a large intrinsic barrier of the electron transfer indicates the occurrence of a significant rearrangement of the bonds and geometries upon the electron-transfer oxidation of organosilanes.

Structural Change Accompanied by Electron-Transfer Oxidation. Clark and Nelsen[32] have recently reported that the AM1 semiempirical MO method provides olefin radical cation geometries

(29) (a) Fukuzumi, S.; Mochizuki, S.; Tanaka, T. *Inorg. Chem.* **1989**, *28*, 2459. (b) Fukuzumi, S.; Koumitsu, S.; Hironaka, K.; Tanaka, T. *J. Am. Chem. Soc.* **1987**, *109*, 305.

(30) The experimental errors in determining the E^0_{ox} values are within ±0.05 V.

(31) The half-wave potential of the enol silyl ether (no. 9) measured by single-sweep voltammetry was reported to be 1.29 V (vs SCE),[6c] which agrees well with the E^0_{ox} value (1.30 V) in Table II.

(32) Clark, T.; Nelsen, S. F. *J. Am. Chem. Soc.* **1988**, *110*, 868.

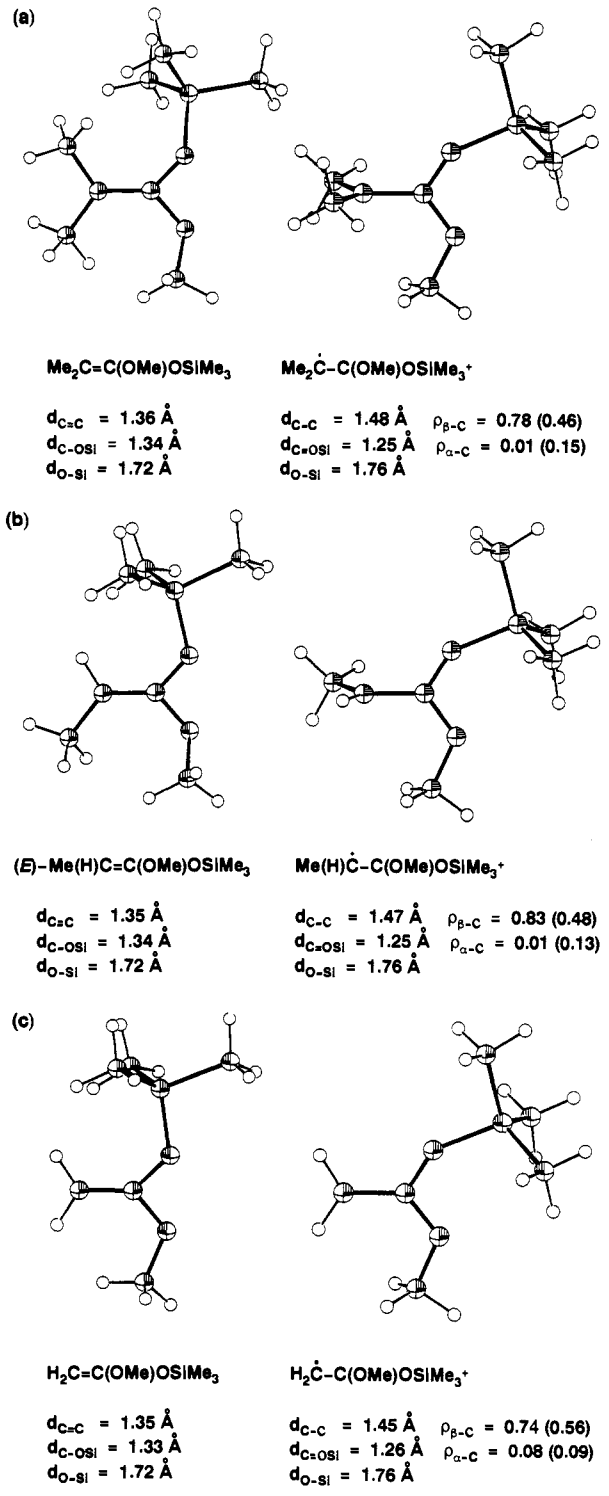

Figure 3. Optimized structures of (a) Me_2C=C(OMe)$OSiMe_3$, (b) (*E*)-Me(H)C=C(OMe)$OSiMe_3$, (c) H_2C=C(OMe)$OSiMe_3$, and the corresponding radical cations, together with the bond lengths and spin densities at the α- and β-carbons ($\rho_{\alpha-C}$ and $\rho_{\beta-C}$) of the radical cations with optimized structures, calculated by using the PM3 method. The values in parentheses are the spin densities of the radical cations with unchanged structures from the neutral form.

in agreement with the observed ESR spectra.[33] Here we performed the latest PM3 semiempirical MO calculations in order to estimate the intrinsic barrier for the electron-transfer oxidation of organosilanes associated with structural change (see the Experimental Section).[15] Figure 3 shows the change in the PM3-optimized structures of a β,β-dimethyl ketene silyl acetal (Me_2C=C(OMe)$OSiMe_3$), a β-monomethyl ketene silyl acetal, and the corresponding radical cations (parts a, b, and c, respectively). With regard to the neutral form of ketene silyl acetals, there is little twist around the ethylenic bond (Figure 3); the siloxy substituent does not confer unusual structural features on the double bond, consistent with the reported crystal structures of a ketene silyl acetal and an enol silyl ether.[34,35] The C=C double bond (1.36 Å) and O—Si single bond (1.72 Å) of Me_2C=C(OMe)$OSiMe_3$ are significantly lengthened in the radical cation (1.48 and 1.76 Å, respectively).[36] The most striking difference between the neutral and radical cation structures of methyl-substituted ketene silyl acetals is that the O—C—O plane which has been coplanar with the Me_2C—C plane in the neutral form turns perfectly perpendicular to this plane upon the formation of a radical cation (Figure 3a,b).[37,38] Such a structural change is also manifested in the change of the SOMO orbitals. The spin of the radical cations with the same structures as the neutral forms is delocalized in the π-orbitals of the two sp^2 carbons as shown in Figure 3 where the spin densities at the α- and β-carbons ($\rho_{\alpha-C}$ and $\rho_{\beta-C}$) are given. The antibonding interaction between the two C=O bonds raises the HOMO level of the neutral form, and an electron may be initially removed from the delocalized π-orbital. In contrast, the spin of the radical cations of methyl-substituted ketene silyl acetals with the optimized structure is mainly localized on the terminal carbon atom (Figure 3a,b), when the positive charge appears mainly on the Si atom (0.82). Thus, the π-radical cation, formed initially by the electron-transfer oxidation of ketene silyl acetals, gets closer to a carbon center radical in the stable form as shown in eq 10. On the other hand, no rotation along the C—C bond occurs in the case of unsubstituted ketene silyl acetals upon electron-transfer oxidation where the spin still remains on the α-carbon (Figure 3c).

$$Me_2C{=}C(OMe)OSiMe_3^{\bullet+} \longleftrightarrow Me_2\dot{C}C(OMe){=}O{\cdots}(\overset{+}{S}iMe_3) \quad (10)$$

Introduction of a bulky substituent by replacing the OMe and $SiMe_3$ groups of Me_2C=C(OMe)$OSiMe_3$ with the O^{t}Bu and $SiMe_2{}^t$Bu groups causes an interesting change in the radical cation structure as shown in Figure 4a. As in the case of Me_2C=C(OMe)$OSiMe_3^{\bullet+}$, lengthening of the C=C double bond and O—Si single bond occurs accompanied by shortening of the C—O bonds. However, no drastic rotation along the C—C bond takes place in the case of Me_2C=C(O^{t}Bu)$OSiMe_2{}^t$Bu$^{\bullet+}$ (Figure 4a). Consequently the spin of the radical cation still remains delocalized in the π-orbitals of the two sp^2 carbons and two oxygen atoms. In the case of the corresponding radical cation of β-monomethyl ketene silyl acetal [(*E*)-Me(H)C=C(O^{t}Bu)$OSiMe_2{}^t$Bu], however, the rotation along the C—C bond occurs and the structural change (Figure 4b) is essentially the same as in the case of (*E*)-Me(H)C=C(OMe)$OSiMe_3$ (Figure 3b).[39] The spin of the radical cation in the stable form is also localized on the terminal carbon atom (Figure 4b). The structural change of H_2C=C(O^{t}Bu)-

(33) (a) Shida, T.; Egawa, Y.; Kubodera, H.; Kato, T. *J. Chem. Phys.* **1980**, *73*, 5963. (b) Shiotani, M.; Nagata, Y.; Sohma, J. *J. Chem. Phys.* **1984**, *88*, 4078. (c) Fujisawa, J.; Sato, S.; Shimokoshi, K.; Shida, T. *J. Phys. Chem.* **1985**, *89*, 5481.

(34) The crystal structure of (*E*)-Me(H)C=C(O^{t}Bu)$OSiPh_2{}^t$Bu has been reported: Babston, R. E.; Lynch, V.; Wilcox, C. S. *Tetrahedron Lett.* **1989**, *30*, 447.

(35) The crystal structure of Ph_2C=C[N(Ph)COEt]$OSiMe_2{}^t$Bu has been reported: Brisse, F.; Thoraval, D.; Chan, T. H. *Can. J. Chem.* **1986**, *64*, 739.

(36) The reported bond lengths of the C=C double bond (1.32 Å) and O—Si single bond (1.66 Å) in the crystal structure of (*E*)-Me(H)C=C(O^{t}Bu)$OSiPh^tBu$[34] are somewhat shorter than the calculated values shown in Figures 3 and 4.

(37) Twisted structures of trimethylsilyl olefin radical cations are well documented on the basis of the ESR spectra; see: Kira, M.; Nakazawa, H.; Sakurai, H. *J. Am. Chem. Soc.* **1983**, *105*, 6983.

(38) A similar conformational change between the neutral and radical cation structures was obtained by using the MNDO method. In this study the PM3 method is preferred to obtain more reliable ΔH_f (heat of formation) values.

(39) For the thermodynamic results for the isomerism in ketene silyl acetals, see: Wilcox, C. S.; Babston, R. E. *J. Org. Chem.* **1984**, *49*, 1451.

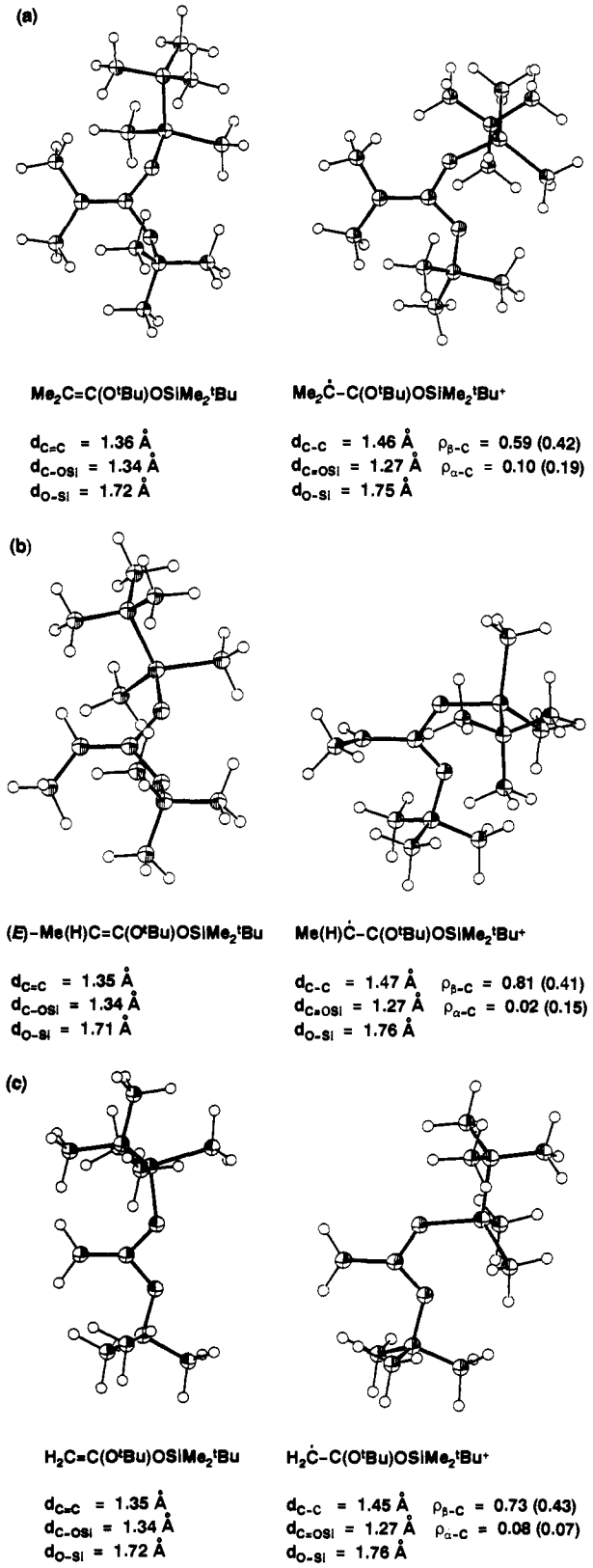

Figure 4. Optimized structures of (a) $Me_2C{=}C(O^tBu)OSiMe_2{}^tBu$, (b) (*E*)-$Me(H)C{=}C(O^tBu)OSiMe_2{}^tBu$, (c) $H_2C{=}C(O^tBu)OSiMe_2{}^tBu$, and the corresponding radical cations, together with the bond lengths and spin densities at the α- and β-carbons ($\rho_{\alpha\text{-}C}$ and $\rho_{\beta\text{-}C}$) of the radical cations, calculated by using the PM3 method. The values in parentheses are the spin densities of the radical cations with unchanged structures from the neutral form.

$OSiMe_2{}^tBu$ upon electron-transfer oxidation (Figure 4c) is similar to that of $H_2C{=}C(OMe)OSiMe_3$ (Figure 3c). Thus, methyl-substituted ketene silyl acetals may be regarded as unique electron donors: they are initially π-donors but are converted to radicals

Table III. Adiabatic Ionization Potentials (I_a) of Organosilanes and Solvation (ΔG_s) and Reorganization Energies (λ_i) of Organosilane Radical Cations Calculated by the PM3 Method

organosilane	I_a, eV	$-\Delta G_s$, kcal mol^{-1}	λ_i, kcal mol^{-1}
$Me_2C{=}C(OMe)OSiMe_3$	7.25	47	12.6
(*E*)-$Me(H)C{=}C(OMe)OSiMe_3$	7.44	46	14.2
$H_2C{=}C(OMe)OSiMe_3$	7.74	47	12.0
$Me_2C{=}C(O^tBu)OSiMe_2{}^tBu$	7.09	39	19.0
(*E*)-$Me(H)C{=}C(O^tBu)OSiMe_2{}^tBu$	7.27	41	14.4
$H_2C{=}C(O^tBu)OSiMe_2{}^tBu$	7.56	42	12.0
$Me_2C{=}CHCH_2SiMe_3$	7.93	49	12.5
$H_2C{=}CHCH_2SiMe_3$	8.42	58	18.0
$PhCH_2SiMe_3$	8.16	55	19.9

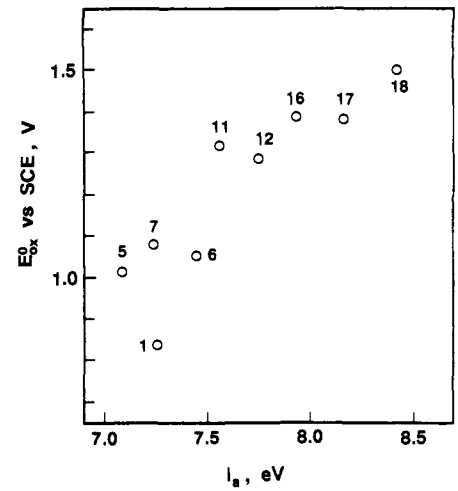

Figure 5. Plot of the one-electron oxidation potentials (E^0_{ox} vs SCE) in Table II vs the adiabatic ionization potentials (I_a) of organosilanes in Table III. The numbers refer to organosilanes in Table II.

that have strong σ-bonding character by electron-transfer oxidation. In this context, it is interesting to note that $Me_2C{=}C(O^tBu)OSiMe_2{}^tBu^{\bullet+}$ preserves the π-radical cation character, while other radical cations become carbon center radicals. Such a difference may be reflected in the reactivities of the radical cations as discussed later.

Significance of Solvation of Radical Cations. Although the vertical ionization potentials (I_v) of some organosilanes have been determined by using photoelectron spectroscopy,[40] no I_v values are available for most of the organosilanes employed in this study. In addition, the I_v values do not contain the effect of structural change upon electron-transfer oxidation. In the case of Me_4Si the value of the adiabatic ionziation potential (I_a) including the structural change accompanied by ionization has been reported to be 9.42 eV, which is significantly smaller than the corresponding I_v value (10.57 eV).[41] Such a large difference between the I_v and I_a values can be well predicted by the calculation using the PM3 method (vide infra). The I_v and I_a values can be calculated as the differences in the heat of formation (ΔH_f) between the neutral form with the optimized structure and the radical cation with the unchanged structure from the optimized neutral form and between the optimized neutral form and the optimized radical cation form using RHF formalism, respectively. The calculated I_v and I_a values were 10.31 and 9.37 eV, which agree well with the experimental values (10.57 and 9.42 eV, respectively). Thus, we calculated the I_a values of typical organosilanes employed in this study using the PM3 method. The difference in ΔH_f of the radical cations with

(40) (a) Pitt, C. G.; Bock, H. *J. Chem. Soc., Chem. Commun.* **1972**, 28. (b) Bock, H.; Kaim, W.; Kira, M.; Osawa, H.; Sakurai, H. *J. Organomet. Chem.* **1979**, *164*, 295. (c) Bock, H.; Kaim, W.; Rohwer, H. E. *J. Organomet. Chem.* **1977**, *135*, C14. (d) Bock, H.; Kaim, W. *J. Am. Chem. Soc.* **1980**, *102*, 4429. (e) Weidner, U.; Schweig, A. *Angew. Chem., Int. Ed. Engl.* **1972**, *11*, 146.

(41) Evans, S.; Green, J. C.; Joachim, P. J.; Orchard, A. F.; Turner, D. W.; Maier, J. P. *J. Chem. Soc., Faraday Trans. 2* **1972**, *68*, 905.

the unchanged structures from the neutral forms and ΔH_f with the optimized structures can be regarded as the rearrangement energy of the inner coordination spheres (λ_i) associated with the structural change upon electron-transfer oxidation in the gas phase.[42] The I_a and λ_i values thus obtained are listed in Table III. Comparison of the I_a values in Table III and the E^0_{ox} values in Table II is shown in Figure 5, where the general trend that E^0_{ox} increases with an increase in I_a is recognized clearly. One may also recognize that the E^0_{ox} values of the ^{t}Bu-substituted ketene silyl acetals are larger than those expected from the correlation between E^0_{ox} and I_a for the other organosilanes (Figure 5). Such a difference may be ascribed to the difference in solvation of the radical cation, since replacement of the Me group by the bulky group (^{t}Bu), which may shield the positive charge center (Si^+) more effectively, may result in the decrease in the solvation energy.

The solvation energy (ΔG_s) for organosilanes attendant upon electron-transfer oxidation is given by the difference between the adiabatic ionization potential in the gas phase and the electron-transfer oxidation in solution (eq 11),[43,44] where C is a constant (4.40 V vs SCE)[45] that includes the potential of the reference electrode on the absolute scale together with the liquid junction potential. The values of the solvation energies of organosilane

$$\Delta G_s/F = E^0_{ox} - I_a + C \qquad (11)$$

radical cations obtained in this manner are also listed in Table III, where the ΔG_s values of radical cations of the ^{t}Bu-substituted ketene silyl acetals are significantly smaller than those of the other ketene silyl acetals. The large ΔG_s values of radical cations of allylsilane derivatives compared with those of ketene silyl acetals (Table III) may be ascribed to the more localized positive charge on the Si atom of allylsilane radical cations than that of ketene silyl acetal radical cations in which the positive charge is partially delocalized on the α-carbon atom.

The intrinsic barrier of electron transfer, $\Delta G^{\ddagger}_0$ in Table II, comprises the reorganization energies for electron-transfer oxidation of organosilanes and electron-transfer reduction of oxidants. Since the reorganization energies for the electron-transfer reduction of oxidants used in this study are known to be relatively small,[19] the large $\Delta G^{\ddagger}_0$ values may be attributed to the large reorganization energies (λ_i) required for the electron-transfer oxidation of organosilanes (Table III). According to the Marcus theory, $\Delta G^{\ddagger}_0$ corresponds to $\lambda/4$ [$=(\lambda + \lambda_0)/4$] in which λ is a composite of the rearrangement energy of the inner coordination spheres (λ_i) associated with structural change and that of the outer coordination spheres (λ_0) associated with solvent reorganization.[24] Although the experimental errors involved in determining the $\Delta G^{\ddagger}_0$ values and the reliability for the calculation of the λ_i values preclude a detailed comparison between $\Delta G^{\ddagger}_0$ and $\lambda_i/4$, the trend that the $\Delta G^{\ddagger}_0$ values (4–5 kcal mol^{-1}) are larger than the corresponding $\lambda_i/4$ values (3–4 kcal mol^{-1}) is unmistakable. The difference between $\Delta G^{\ddagger}_0$ and $\lambda_i/4$ indicates that solvent reorganization also plays an important role in determining the intrinsic barrier of the electron-transfer oxidation of organosilanes, consistent with the large solvation energies of the radical cations (Table III).

Mechanistic Insight into Lewis Acid Mediated Reactions. In our recent communication, we disclosed that Lewis acid mediated electron transfer plays a key role in the Mukaiyama–Michael reactions of ketene silyl acetals, particularly in the cases of the reactions of sterically hindered derivatives, such as β,β-dimethyl ketene silyl acetals with a hindered α-enone, thus allowing the smooth connection of contiguous quaternary carbon centers which would otherwise be difficult to achieve (eq 12).[8,46] The unique

$$Me_2C{=}C(OEt)OSiEt_3 + Me_2C{=}C(H)COPh \xrightarrow{\text{Lewis acid}} PhCOCH_2CMe_2CMe_2COOEt \qquad (12)$$

donor properties described above, such that initial π-donors are converted to carbon-centered radicals by electron-transfer oxidation, now offer an excellent opportunity to develop more mechanistic insight into the synthetically useful reaction (vide infra).

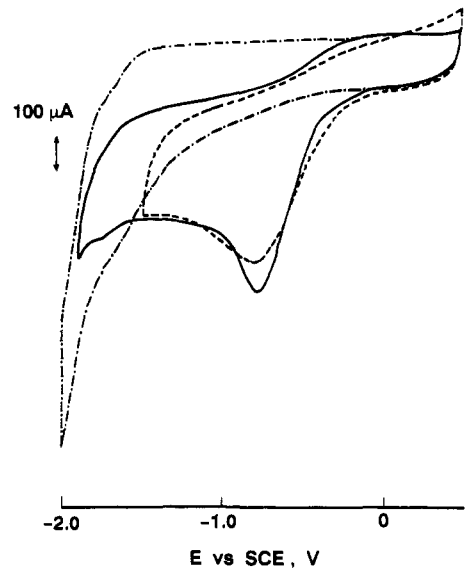

Figure 6. Cyclic voltammograms of a CH_2Cl_2 solution containing a mixture of $Me_2C{=}C(H)COPh$ (1.0×10^{-2} M) and Et_3SiClO_4 (5.0×10^{-3} M) (—), $Me_2C{=}C(H)COPh$ (---), or Et_3SiClO_4 (···) in the presence of Bu_4NClO_4 (5.0×10^{-2} M) at the sweep rate of 100 mV s^{-1}.

Lewis acids which are usually employed in the Mukaiyama reaction were not regarded as strong one-electron oxidants.[47] Yet ferrocene ($Fe(C_5H_5)_2$), a mild one-electron reductant, has proved to be readily oxidized by $SnCl_4$, Ph_3SiClO_4, and Et_3SiClO_4 to yield ferrocenium ion in CH_2Cl_2 at 298 K (k_{et} = 0.72, 0.21, and 1.0 $\times 10^{-2}$ M^{-1} s^{-1}, respectively). As expected from the energetics of electron transfer, the k_{et} values of Et_3SiClO_4 increase with a decrease in the E^0_{ox} values of ferrocene derivatives (2.2×10^{-1} and 6.8×10^3 M^{-1} s^{-1} for $Fe(MeC_5H_4)_2$ and $Fe(Me_5C_5)_2$, respectively). On the other hand, Tanner et al. have recently reported that no electron transfer from $Fe(C_5H_5)_2$ to Bu_3SnClO_4 or $PhSnClO_4$ takes place, but that it does occur from the stronger reductant $Fe(Me_5C_5)_2$ to Bu_3SnClO_4 and Ph_3SnClO_4 with rate constants 2.9 and 19 M^{-1} s^{-1}, respectively.[48] Thus, the oxidizing ability of these Lewis acids is in the order $SnCl_4 > Ph_3SiClO_4 > Et_3SiClO_4 > Ph_3SnClO_4 > Bu_3SnClO_4$.

Since the hindered ketene silyl acetals can transfer an electron to $Fe(C_5H_5)_2^+$ efficiently and $Fe(C_5H_5)_2$ does so to the Lewis acids, electron transfer from the hindered ketene silyl acetals to Lewis acids is energetically allowed to occur. On the other hand, no electron transfer has taken place from $Fe(C_5H_5)_2$ to the enone, while electron-transfer oxidation of $Fe(C_5H_5)_2$ does take place with Lewis acids even in the presence of an excess amount of $Me_2C{=}C(H)COPh$.[49] The rates were somewhat diminished by the presence of α-enone, suggestive of interaction between the Lewis acid and the α-enone (for example, $k_{et} = 1.6 \times 10^{-3}$ M^{-1}

(42) The small λ_i value that is equal to the difference in the I_v and I_a values has been reported for the ionization of styrene (0.10 eV): Maier, J. P.; Turner, D. W. *Faraday Discuss. Chem. Soc.* **1972**, *54*, 149. The calculated λ_i value (0.17 eV) using the PM3 method agrees well with the experimental λ_i value.

(43) (a) Peover, M. E. *Electroanal. Chem.* **1967**, *2*, 1. (b) Fukuzumi, S.; Kochi, J. K. *J. Am. Chem. Soc.* **1982**, *104*, 7599.

(44) The solvation of the neutral species is neglected in comparison with the corresponding radical cation.

(45) Larson, R. C.; Iwamoto, R. T.; Adams, R. N. *Anal. Chim. Acta* **1961**, *25*, 371. The value of C for the $Ag/AgClO_4$ reference in MeCN is 4.70 V, which is decreased by 0.30 V when related to the SCE reference.

(46) No free radicals escaping from the cage may be involved in the reaction, since no homocoupling products have been detected.[8]

(47) One-electron reduction of strong Lewis acids such as $AlCl_3$ and $SbCl_5$ is well-known: Bard, A. J.; Ledwith, A.; Shine, H. J. *Adv. Phys. Org. Chem.* **1976**, *13*, 155.

(48) Tanner, D. D.; Harrison, D. J.; Chen, J.; Kharrat, A.; Wayner, D. D. M.; Griller, D.; McPhee, D. J. *J. Org. Chem.* **1990**, *55*, 3321.

(49) The cyclic voltammogram of the α-enone indicated that the reduction in CH_2Cl_2 occurred at largely negative electrode potential, E (vs SCE) < -1.7 V, as shown in Figure 6, and thus electron transfer from $Fe(C_5H_5)_2$ to the enone is highly endergonic.

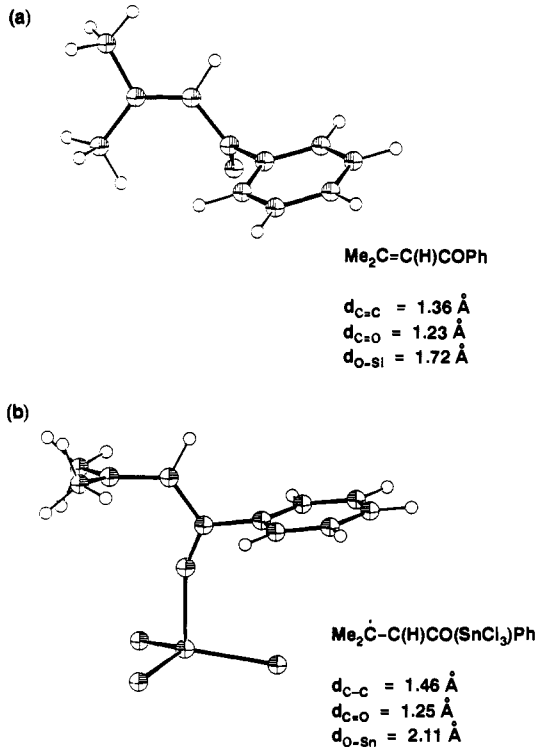

Figure 7. Optimized structures of (a) $Me_2C{=}C(H)COPh$ and (b) $Me_2C^{\bullet}{-}C(H)CO(SnCl_3)Ph$, together with bond lengths, calculated by using the MNDO method.

s^{-1} in CH_2Cl_2 at 298 K with $SnCl_4$). Nevertheless, such an interaction may not be strong enough to change the susceptibility to electron-transfer reduction of both components, since the cathodic peak potentials observed in the cyclic voltammograms of the α-enone–Et_3SiClO_4 system in CH_2Cl_2 exhibited no appreciable changes as compared with those of the superposition of each component as shown in Figure 6. No significant change in the cyclic voltammograms was observed for the cathodic reduction of $SnCl_4$ in the presence of α-enone as compared with that in its absence either. Thus, electron transfer from the hindered ketene silyl acetals may occur initially to Lewis acid rather than to α-enone. Since the electron-transfer reduction of $SnCl_4$ undergoes spontaneous fragmentation to $^{\bullet}SnCl_3$ and Cl^-,[50] $^{\bullet}SnCl_3$ thus formed may add to α-enone to give a stannyl enolate radical.

Figure 7 shows the change of the MNDO-optimized structures from α-enone $Me_2C{=}C(H)COPh$ to the corresponding stannyl enolate radical (parts a and b, respectively). The structural change between the α-enone and the stannyl enolate radical in Figure 7 is essentially the same as seen in Figures 3 (parts a and b) and 4 (part b), i.e., the addition of $^{\bullet}SnCl_3$ radical to α-enone results in rotation along the C—C bond and the two coplanar sp^2 planes become perpendicular to each other.[51-53] Consequently, electron transfer from the hindered ketene silyl acetal to the hindered α-enone may result in the formation of two carbon-centered radicals which are coupled together in the cage.[46] This may be the reason why Lewis acid mediated electron transfer allows smooth connection of contiguous quaternary carbon centers which would otherwise be difficult to achieve (eq 12).

In general, β-substitution of ketene silyl acetals increases the steric hindrance of the reaction center, thereby reducing the reactivity of nucleophilic attack toward electrophiles. On the other hand, the same β-substitution increases the electron donor ability to become more susceptible to electron-transfer oxidation. Extension of these two reverse effects leads one to expect the mechanistic change from ubiquitous S_N2 processes to electron-transfer processes. It is hoped that the present study has provided fundamental properties for the electron-transfer oxidation of various organosilanes required to exploit the expanding scope of electron-transfer oxidation as well as to differentiate the dichotomy of S_N2 and electron-transfer processes.

Acknowledgment. This work was partially supported by a grant-in-aid from the Ministry of Education, Science, and Culture, Japan.

(50) (a) Chanon, M.; Rajzmann, M.; Chanon, F. *Tetrahedron* **1990**, *46*, 6193. (b) Symons, M. C. R. *Pure Appl. Chem.* **1981**, *53*, 223.

(51) The calculated ΔH_f value of the stannyl enolate radical (−86 kcal mol^{-1}) is slightly larger than the sum of the ΔH_f values of $^{\bullet}SnCl_3$ and $Me_2C{=}C(H)COPh$ (−88 kcal mol^{-1}). Thus, the adduct formation of $^{\bullet}SnCl_3$ to the α-enone may be reversible. This accounts well for the *E*–*Z* isomerization of the α-enone [Me(Et)C=C(H)OPh] occurring during the Mukaiyama–Michael reaction.[8]

(52) Although the stannyl enolate radical has not been detected, the ESR spectrum of the complex formed between a stable acrylate radical and $SnCl_4$ has been reported: Tanaka, H.; Sakai, I.; Ota, T. *J. Am. Chem. Soc.* **1986**, *108*, 2208.

(53) The weak conjugation of the carbonyl group to the phenyl group as seen in Figure 7 has often been observed in the crystal structures of acrylophenone derivatives and benzoyl compounds: Follet-Houttemane, P. C.; Wignacourt, J. P.; Boivin, J. C.; Lesieur, I.; Lesieur, D. *Acta Crystallogr.* **1991**, *C47*, 602. Knapp, S.; Toby, B. H.; Sebastian, M.; Krogh-Jespersen, K.; Potenza, J. A. *J. Org. Chem.* **1981**, *46*, 2490. LaLonde, R. T.; Florence, R. A.; Horenstein, B. A.; Fritz, R. C.; Silveira, L.; Clardy, J.; Krishnan, B. S. *J. Org. Chem.* **1985**, *50*, 85.